AMERICAN SOCIETY FOR MICROBIOLOGY | Antimicrobial Agents and Chemotherapy®

PHARMACOLOGY

In Vitro and *In Vivo* Assessment of FK506 Analogs as Novel Antifungal Drug Candidates

Yeonseon Lee,[a] Kyung-Tae Lee,[a] Soo Jung Lee,[a] Ji Yoon Beom,[b] Areum Hwangbo,[a] Jin A Jung,[b] Myoung Chong Song,[b] Young Ji Yoo,[c] Sang Hyeon Kang,[c] Anna F. Averette,[d,e,f] Joseph Heitman,[d,e,f] Yeo Joon Yoon,[b] Eunji Cheong,[a] Yong-Sun Bahn[a]

[a]Department of Biotechnology, College of Life Science and Biotechnology, Yonsei University, Seoul, Republic of Korea

[b]Department of Chemistry and Nanoscience, Ewha Womans University, Seoul, Republic of Korea

[c]iNtRON Biotechnology, Inc., Seongnam-si, Gyeonggi-do, Republic of Korea

[d]Department of Molecular Genetics and Microbiology, Duke University Medical Center, Durham, North Carolina, USA

[e]Department of Medicine, Duke University Medical Center, Durham, North Carolina, USA

[f]Department of Pharmacology and Cancer Biology, Duke University Medical Center, Durham, North Carolina, USA

ABSTRACT FK506 (tacrolimus) is an FDA-approved immunosuppressant indicated for the prevention of allograft rejections in patients undergoing organ transplants. In mammals, FK506 inhibits the calcineurin-nuclear factor of activated T cells (NFAT) pathway to prevent T-cell proliferation by forming a ternary complex with its binding protein, FKBP12, and calcineurin. FK506 also exerts antifungal activity by inhibiting calcineurin, which is essential for the virulence of human-pathogenic fungi. Nevertheless, FK506 cannot be used directly as an antifungal drug due to its immunosuppressive action. In this study, we analyzed the cytotoxicity, immunosuppressive activity, and antifungal activity of four FK506 analogs, 31-*O*-demethyl-FK506, 9-deoxo-FK506, 9-deoxo-31-*O*-demethyl-FK506, and 9-deoxo-prolyl-FK506, in comparison with that of FK506. The four FK506 analogs generally possessed lower cytotoxicity and immunosuppressive activity than FK506. The FK506 analogs, except for 9-deoxo-prolyl-FK506, had strong antifungal activity against *Cryptococcus neoformans* and *Candida albicans*, which are two major invasive pathogenic yeasts, due to the inhibition of the calcineurin pathway. Furthermore, the FK506 analogs, except for 9-deoxo-prolyl-FK506, had strong antifungal activity against the invasive filamentous fungus *Aspergillus fumigatus*. Notably, 9-deoxo-31-*O*-demethyl-FK506 and 31-*O*-demethyl-FK506 exhibited robust synergistic antifungal activity with fluconazole, similar to FK506. Considering the antifungal efficacy, cytotoxicity, immunosuppressive activity, and synergistic effect with commercial antifungal drugs, we selected 9-deoxo-31-*O*-demethyl-FK506 for further evaluation of its *in vivo* antifungal efficacy in a murine model of systemic cryptococcosis. Although 9-deoxo-31-*O*-demethyl-FK506 alone was not sufficient to treat the cryptococcal infection, when it was used in combination with fluconazole, it significantly extended the survival of *C. neoformans*-infected mice, confirming the synergistic *in vivo* antifungal efficacy between these two agents.

KEYWORDS calcineurin, FKBP12, human fungal pathogen, calcium signaling, immunosuppressant

Fungal infections are emerging as a global threat to plant and animal ecosystems due to a number of natural, environmental, and/or artificial factors, causing species extinction and endangering agriculture and food security (1–3). The impact of mycoses, fungal infections of animals, on human health is generally poorly appreciated by the public but cannot be overlooked. Recent epidemiological studies have reported that almost one-quarter of the human population has superficial infections of the skin and

Received 1 August 2018 **Returned for modification** 18 August 2018 **Accepted** 26 August 2018

Accepted manuscript posted online 4 September 2018

Citation Lee Y, Lee K-T, Lee SJ, Beom JY, Hwangbo A, Jung JA, Song MC, Yoo YJ, Kang SH, Averette AF, Heitman J, Yoon YJ, Cheong E, Bahn Y-S. 2018. *In vitro* and *in vivo* assessment of FK506 analogs as novel antifungal drug candidates. Antimicrob Agents Chemother 62:e01627-18. https://doi.org/10.1128/AAC.01627-18.

Address correspondence to Joseph Heitman, heitm001@duke.edu, Yeo Joon Yoon, joonyoon@ewha.ac.kr, Eunji Cheong, eunjicheong@yonsei.ac.kr, or Yong-Sun Bahn, ysbahn@yonsei.ac.kr.

Y.L., K.-T.L., S.J.L., and J.Y.B. contributed equally to this article.

nails, including athlete's foot and ringworm (tinea), primarily caused by dermatophytes (4). Nevertheless, in general, superficial mycoses are not life-threatening. In contrast, invasive mycoses, which occur at a lower incidence than superficial mycoses, impose a more serious threat to human health and are associated with a high rate of mortality (4). More than 2 million invasive fungal infections are estimated to occur globally every year and are responsible for more than 1 million deaths, particularly in immunocompromised individuals. Approximately 90% of invasive mycoses are caused by four opportunistic fungal pathogens: *Aspergillus fumigatus*, *Candida albicans*, *Cryptococcus neoformans*, and *Pneumocystis jirovecii*. Moreover, the incidence of invasive mycoses is expected to increase in the future, due to an increase in the population of immunocompromised individuals resulting from the increased human life span and a variety of immunosuppressive diseases (e.g., AIDS) and medical treatments, such as solid organ transplantation and anticancer chemotherapy (5–7).

Regardless of the ecological, agricultural, and clinical importance of fungal infections, antifungal treatment options are limited compared with antibacterial treatment options, mainly due to the eukaryotic structure of fungal cells, which is similar to that of plant and animal cells. The first antifungal agents developed were the polyenes, such as amphotericin B and nystatin. These amphiphilic macrocyclic chemicals bind to sterols in the fungal cell membrane, resulting in the formation of lethal pores, which allow leakage of essential intracellular ions and small organic molecules (8). However, polyenes result in nephrotoxicity and other toxic effects (9, 10). The most commonly used antifungal agents are the azoles, such as imidazoles (e.g., ketoconazole) and triazoles (e.g., fluconazole, itraconazole, voriconazole). Azoles inhibit lanosterol 14α-demethylase (Erg11), which causes cells to accumulate toxic sterol precursors in the fungal cell membrane, perturbing membrane integrity. However, azoles generally exhibit only fungistatic effects and hepatotoxicity (11). Allylamines (e.g., terbinafine) inhibit squalene epoxidase (Erg1), which catalyzes the first step in ergosterol biosynthesis, and are generally used as topical agents for the treatment of superficial mycoses (12). Flucytosine, which is a 5-fluorinated cytosine analog, inhibits the salvage pathway for pyrimidine biosynthesis, hampering DNA and RNA synthesis. This agent is normally used in combination with amphotericin B. However, flucytosine exhibits hematological toxicity, and resistance occurs readily (13). Echinocandins (e.g., caspofungin, micafungin) inhibit β-(1,3)-glucan synthase and perturb fungal cell wall integrity. Although the side effects associated with the use of echinocandins are less severe than those associated with the use of other antifungal agents, their antifungal spectrum is narrow and their use may also lead to hepatotoxicity following long-term administration (14–16). Nevertheless, all of these antifungal agents are associated with toxicity, a lack of efficacy, a limited spectrum of activity, frequent resistance, and restrictions due to the administration route and/or the bioavailability of target tissues (17). Therefore, extensive efforts have been made to develop novel antifungal agents (18).

Among a number of novel antifungal drug candidates, FK506 (tacrolimus) has received much attention owing to its strong antifungal activity against a broad spectrum of fungal pathogens (19–21). In humans, FK506 is a widely used immunosuppressant similar to cyclosporine (CsA), forms a complex with the FK506 binding protein FKBP12, and subsequently blocks activation of the calcineurin pathway (22). Inactivation of calcineurin, a calcium- and calmodulin-dependent serine/threonine protein phosphatase, prevents the dephosphorylation and activation of calcineurin-nuclear factor of activated T cells (NFAT), thereby inhibiting the expression of interleukin-2 and subsequent T-cell proliferation (23, 24). Notably, the calcineurin pathway also plays pivotal roles in plant and animal fungal pathogens (25, 26). In *C. neoformans*, which causes fatal systemic cryptococcosis and meningoencephalitis (27), the calcineurin pathway is required for maintenance of cell wall integrity and survival at mammalian body temperature (28). In *C. albicans*, which causes both superficial and systemic candidiasis (29), calcineurin is required for survival in the presence of serum (30–33). In *A. fumigatus*, which causes life-threatening systemic and invasive aspergillosis (34), the calcineurin pathway regulates conidial germination and hyphal growth (35). In human

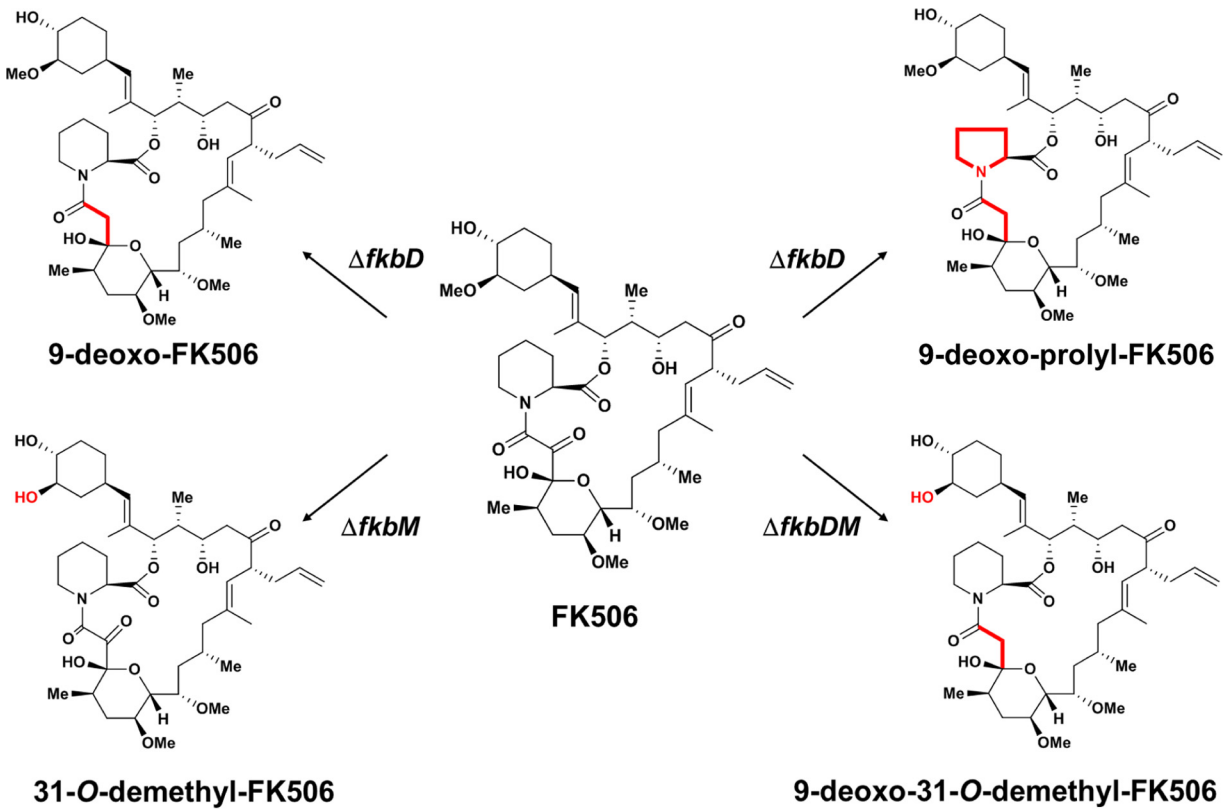

FIG 1 Chemical structures of FK506 and its analogs used in this study. Modifications to the FK506 structure are highlighted in red (39, 40).

fungal pathogens, deletion of calcineurin genes considerably attenuates their infectivity and virulence (36).

Despite its potent antifungal activity, FK506 cannot be used directly as an antifungal agent due to its strong immunosuppressive activity. Therefore, substantial efforts have been made to chemically develop FK506 analogs with a reduced ability to inhibit T cells but with retained antifungal activity (37). Furthermore, combinatorial biosynthetic approaches involving manipulation of the FK506 biosynthetic genes have been widely employed to generate diverse FK506 analogs with improved or altered biological properties in several *Streptomyces* species, including *Streptomyces clavuligerus*, *Streptomyces kanamyceticus*, and *Streptococcus tsukubaensis* (38). Previously, we generated 31-*O*-demethyl-FK506 (31OD-FK506) by deleting the *fkbM* gene, which is involved in the 31-*O*-methylation of FK506, and 9-deoxo-31-*O*-demethyl-FK506 (9D31OD-FK506) by deleting the *fkbD* gene, which is responsible for C-9 oxidation, and the *fkbM* gene (39). We also reported the biosynthesis of 9-deoxo-FK506 (9D-FK506) and 9-deoxo-prolyl-FK506 (9DP-FK506) following deletion of the *fkbD* gene in the FK506 biosynthetic pathway. Interestingly, the *in vitro* immunosuppressive activity of 9DP-FK506 was significantly reduced, while *in vitro* neuroregenerative activity was only slightly reduced (40). These results suggest the potential of structural modifications of FK506 for the development of improved biological agents.

In this study, we examined the *in vitro* and *in vivo* antifungal efficacy of four FK506 analogs, including 9D-, 9DP-, 31OD-, and 9D31OD-FK506 (Fig. 1), and measured their cytotoxicity and ability to inhibit T-cell proliferation to assess these FK506 analogs for their potential as antifungal drugs. For antifungal efficacy testing, we used three major human pathogens: *C. neoformans*, *C. albicans*, and *A. fumigatus*. Furthermore, we also tested the synergistic effect of each FK506 analog with clinically available antifungal drugs to assess potential combination therapeutic options with the FK506 analogs (40, 41).

RESULTS

Evaluation of the immunosuppressive effect of FK506 analogs. The major hurdle to the use of FK506 as an antifungal drug is its immunosuppressive activity. Therefore, here, we first investigated the immunosuppressive activity of FK506 and its analogs by measuring their effect on the viability and proliferation of primary murine $CD4^+$ helper T cells, because $CD4^+$ helper T cells are essential for adaptive immunity by the release of cytokines, which activate other immune cells (42). $CD4^+$ helper T cells were isolated from the forward scatter area (FSC-A) and side scatter area (SSC-A) at over 95% purity from lymphocyte populations extracted from spleens and were then further analyzed to identify live/dead (L/D) cells. The live/dead percentage of T cells was assessed in the presence of various concentrations of FK506. The percentage of live cells was reduced to about 50% with the presence of FK506 at concentrations higher than 1 ng/ml (Fig. 2A; see also Fig. S1 in the supplemental material), indicating T-cell cytotoxicity. All FK506 analogs exhibited lower levels of T-cell cytotoxicity than FK506 (Fig. 2B). At the highest tested concentration of 1 μg/ml, 9DP-FK506 displayed the lowest toxicity (80% viable cells), followed by 9D31OD-FK506 (76% viable cells), 31OD-FK506 (75% viable cells), and 9D-FK506 (50% viable cells), whereas FK506 displayed the highest toxicity (Fig. 2B).

The immunosuppressive activity of FK506 and its analogs was assessed by monitoring $CD4^+$ T-cell proliferation 72 h after activation by an antigen-like activator (Fig. 2C). Cellular proliferation, monitored by the use of Cell Trace Violet (CTV), was analyzed in the presence of FK506 and its analogs. Cells not activated by the antigen-like activator were used as the negative-control group. The level of proliferation dropped significantly at 0.1 ng/ml of FK506, confirming its potent immunosuppressive activity, whereas no significant change in the proliferation level was observed at the same concentration of the four FK506 analogs (Fig. 2C; see also Fig. S1 in the supplemental material). FK506 presented the lowest 50% inhibitory concentration (IC_{50}) (0.0269 ng/ml), followed by 31OD-FK506 (IC_{50} = 0.2458 ng/ml; 9-fold reduction), 9D-FK506 (IC_{50} = 0.5134 ng/ml; 19-fold reduction), 9D31OD-FK506 (IC_{50} = 15.0900 ng/ml; 561-fold reduction), and 9DP-FK506 (IC_{50} = 268.3000 ng/ml; 9,974-fold reduction) (Fig. 2D). Taken together, all four FK506 analogs resulted in T-cell cytotoxicity and immunosuppressive activity significantly lower than those of FK506.

The FK506 analogs exhibit potent *in vitro* antifungal activity by inhibiting the calcineurin pathway in *C. neoformans*. We first examined the *in vitro* antifungal activity of the four FK506 analogs against *C. neoformans*. To determine antifungal activity in a qualitative manner, we performed a disk diffusion assay using the serotype A *C. neoformans* H99 strain (a genome sequencing platform strain) treated with 0.1, 1, and 10 μg/ml of FK506 and its analogs, and a zone of inhibition was observed after incubation at both 30 and 37°C. As previously shown (43), FK506 inhibited the growth of *C. neoformans* at 37°C but not at 30°C (Fig. 3A). Similarly, the FK506 analogs, except for 9DP-FK506, exhibited anticryptococcal activity in a dose-dependent manner at 37°C but not at 30°C, albeit to a lesser extent than FK506 (Fig. 3A). Among the FK506 analogs, 31OD-FK506 displayed the strongest antifungal activity, whereas 9D-FK506 and 9D31OD-FK506 showed almost equivalent activity. To quantitatively measure the antifungal activity of the FK506 analogs, we determined the average 50% inhibitory concentration (IC_{50}) with nine clinical isolates of *C. neoformans* using the broth microdilution method in RPMI liquid medium at 37°C (instead of the standard 35°C) (Fig. 3B; see also Table S1 in the supplemental material). Similar to the qualitative measurement, FK506 showed the lowest IC_{50} (0.0007 μg/ml), followed by 9D-FK506 (0.0016 μg/ml; 2.3-fold reduction), 31OD-FK506 (0.0018 μg/ml; 2.6-fold reduction), 9D31OD-FK506 (0.0026 μg/ml; 3.7-fold reduction), and 9DP-FK506 (>12.5 μg/ml) (Fig. 3B).

To address whether the antifungal activity of the FK506 analogs was mediated through inhibition of the calcineurin pathway, we examined the susceptibility of the FKBP12 mutant (the *frr1*Δ mutant) to the FK506 analogs. As previously reported (44), the *frr1*Δ mutant was completely resistant to FK506 at 37°C (Fig. 3C). Similarly, the *frr1*Δ

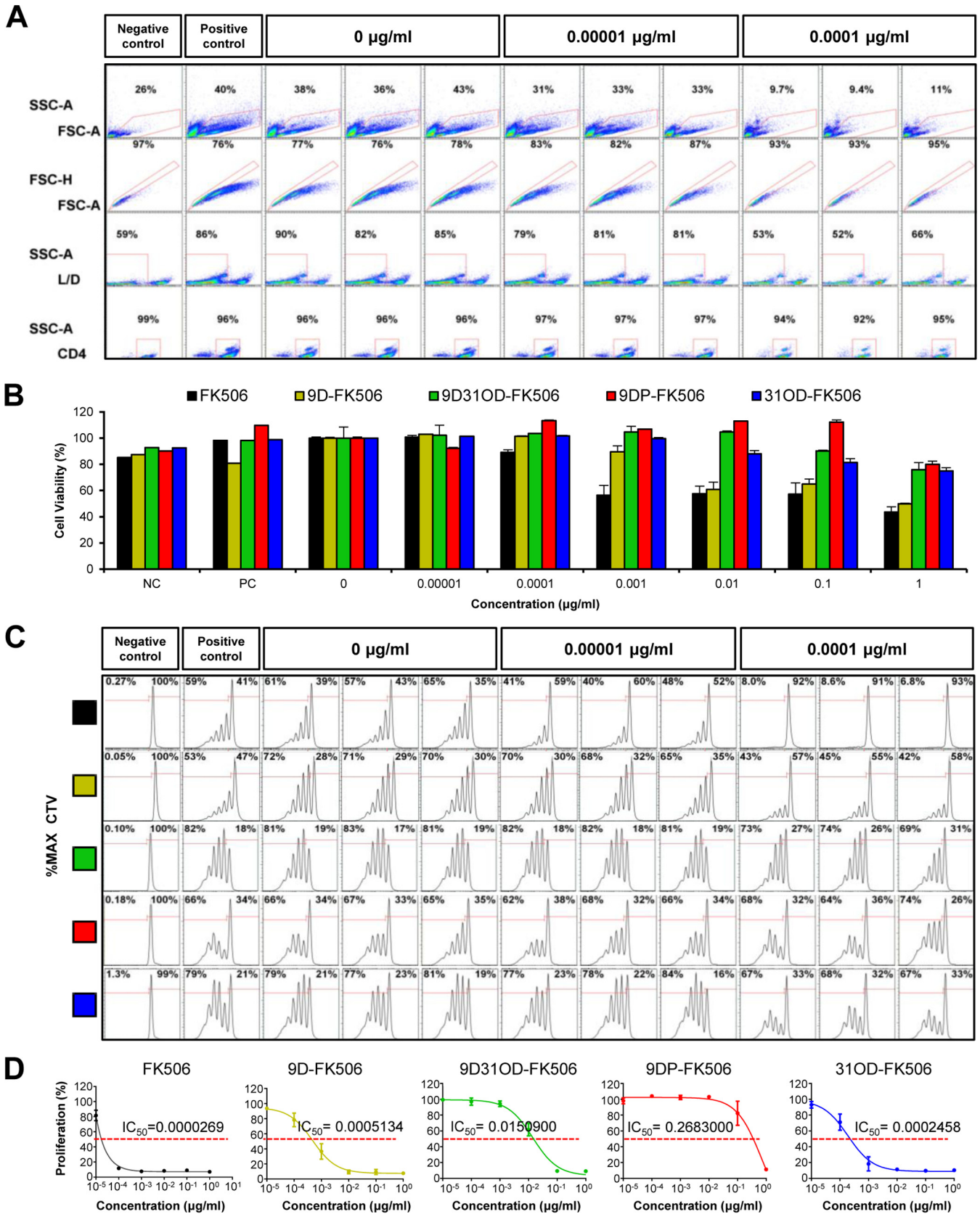

FIG 2 The immunosuppressive effect of the FK506 analogs was reduced compared with that of FK506. (A) The immunosuppressive effect of FK506 on primary $CD4^+$ T helper cells was assessed at various concentrations of FK506 with three replicates using flow cytometry. (First row) Lymphocytes were selected within the boundaries from the forward scatter area (FSC-A) and side scatter area (SSC-A); (2nd row) single cells (within the red box) were selected from the forward

(Continued on next page)

mutant was completely resistant to all four FK506 analogs (Fig. 3C), indicating that the FK506 analogs target FKBP12 in *C. neoformans* similarly to FK506. To further show that the FK506 analogs inhibit the calcineurin pathway in *C. neoformans*, we examined two calcineurin-dependent phenotypic traits. It has previously been shown that deletion of calcineurin (the *cna1*Δ and *cnb1*Δ mutants) renders *C. neoformans* highly defective in terms of cell wall integrity and resistance to the endoplasmic reticulum stress agent tunicamycin (TM) (45). Supporting this, we found that treatment with FK506, 31OD-FK506, 9D-FK506, or 9D31OD-FK506 made wild-type *C. neoformans* more susceptible to TM, as the *cna1*Δ and *cnb1*Δ mutants were more susceptible to TM (Fig. 3D). 9DP-FK506 had only a minor effect on TM resistance (Fig. 3D). In addition, it has previously been shown that FK506 can efficiently kill *C. neoformans*, even at 30°C, when combined with fludioxonil, which is a phenylpyrrole class of fungicide (46). Similarly, 31OD-FK506, 9D-FK506, and 9D31OD-FK506, but not 9DP-FK506, could kill *C. neoformans* at 30°C when combined with fludioxonil (Fig. 3E). This synergism between the FK506 analogs and fludioxonil was dependent on Hog1 and Cna1 (Fig. 3E). Taken together, these results strongly suggest that the FK506 analogs, except for 9DP-FK506, have strong antifungal activity against *C. neoformans* due to the inhibition of the calcineurin pathway.

FK506 analogs exhibit potent *in vitro* antifungal activity by inhibiting the calcineurin pathway in *C. albicans*. We next examined the *in vitro* antifungal activity of the four FK506 analogs against *C. albicans*. Previously, FK506 treatment was shown to increase the susceptibility of *C. albicans* (strain SC5314) to serum (31, 33, 47). To qualitatively examine the serum-mediated antifungal activity of the four FK506 analogs, we performed spot assays with serially diluted SC5134 cells on solid 50% fetal bovine serum (FBS) agar medium (Fig. 4A). Consistent with previous reports (33, 47), the survival of wild-type *C. albicans* (SC5314) cells was greatly reduced following FK506 treatment (3 μg/ml) on solid 50% FBS agar medium; the levels of inhibition were similar to those obtained following deletion of both copies of the *CNB1* gene (DAY364 strain; *cnb1*Δ/*cnb1*Δ), which encode the regulatory subunit of calcineurin in *C. albicans* (Fig. 4A). Mutation of FK506 binding sites in calcineurin (YAG237 strain; *CNB1-1/CNB1*) or disruption of both copies of the FKBP12 gene (YAG171 strain; *rbp1*Δ/*rbp1*Δ) also abolished the serum-mediated antifungal activity of FK506 (Fig. 4A). Among the FK506 analogs, 31OD-FK506 exhibited similar levels of serum-mediated antifungal activity as FK506, whereas 9D-FK506 and 9D31OD-FK506 presented reduced activity (Fig. 4A). In contrast, 9DP-FK506 did not have any such activity, even at 10 μg/ml (Fig. 4A). Similar to FK506, the serum-mediated antifungal activity of 31OD-FK506, 9D-FK506, and 9D31OD-FK506 was not seen in the *CNB1-1/CNB1* and *rbp1*Δ/*rbp1*Δ strains. These results indicate that the serum-mediated antifungal activity of the FK506 analogs in *C. albicans* also results from inhibition of the calcineurin pathway.

To quantitatively measure the serum-mediated antifungal activity of the FK506 analogs, we performed a 2,3-bis-(2-methoxy-4-nitro-5-sulfophenyl)-2*H*-tetrazolium-5-carboxanilide salt (XTT) reduction assay with seven clinical *C. albicans* strains (Table S1). As the XTT reduction assay monitored cell viability by measuring mitochondrial activity, we were able to avoid problems associated with inconsistent measurements of the

FIG 2 Legend (Continued)

scatter height (FSC-H) and forward scatter area (FSC-A) for further analysis; (3rd row) primary cultured T cells from mice were stained with LIVE/DEAD cell viability kits, and the percentage of live cells was determined in the presence of various concentrations of FK506; (4th row) $CD4^+$ helper T cells were isolated with CD4 T-cell enrichment kits. The assay included a negative-control group with inactivated T cells (NC), a positive-control group with activated T cells (PC), and a vehicle group with activated T cells and a concentration of 0 μg/ml. (B) The cytotoxicity of FK506 and its analogs is shown by the percentage of live cells treated with 0.00001 to 1 μg/ml FK506 and its analogs normalized to the number of live cells treated with vehicle. FK506 at 0.001 μg/ml significantly reduced cell viability by ~50%, whereas none of the FK506 analogs at the same concentration showed any cytotoxicity. (C) CellTrace Violet (CTV) was used to dye the cells immediately following culture, and intensity levels were measured to detect proliferation after 72 h of drug exposure. The experiment was performed with three replicates for each concentration of each analog compound tested across a range of concentrations. Multiple peaks indicating the proliferation of T cells diminished at concentrations associated with immune suppression. The percentage of proliferating cells within each group was normalized to the number of cells treated with the vehicle. (D) Data from three independent biological groups were used to calculate the IC_{50} for each compound using nonlinear regression fit analysis. Curves for all compounds displayed higher IC_{50}s compared with the IC_{50} of FK506, which indicated a significant reduction in immunosuppressive activity. All data are presented as the mean ± standard error of the mean (SEM).

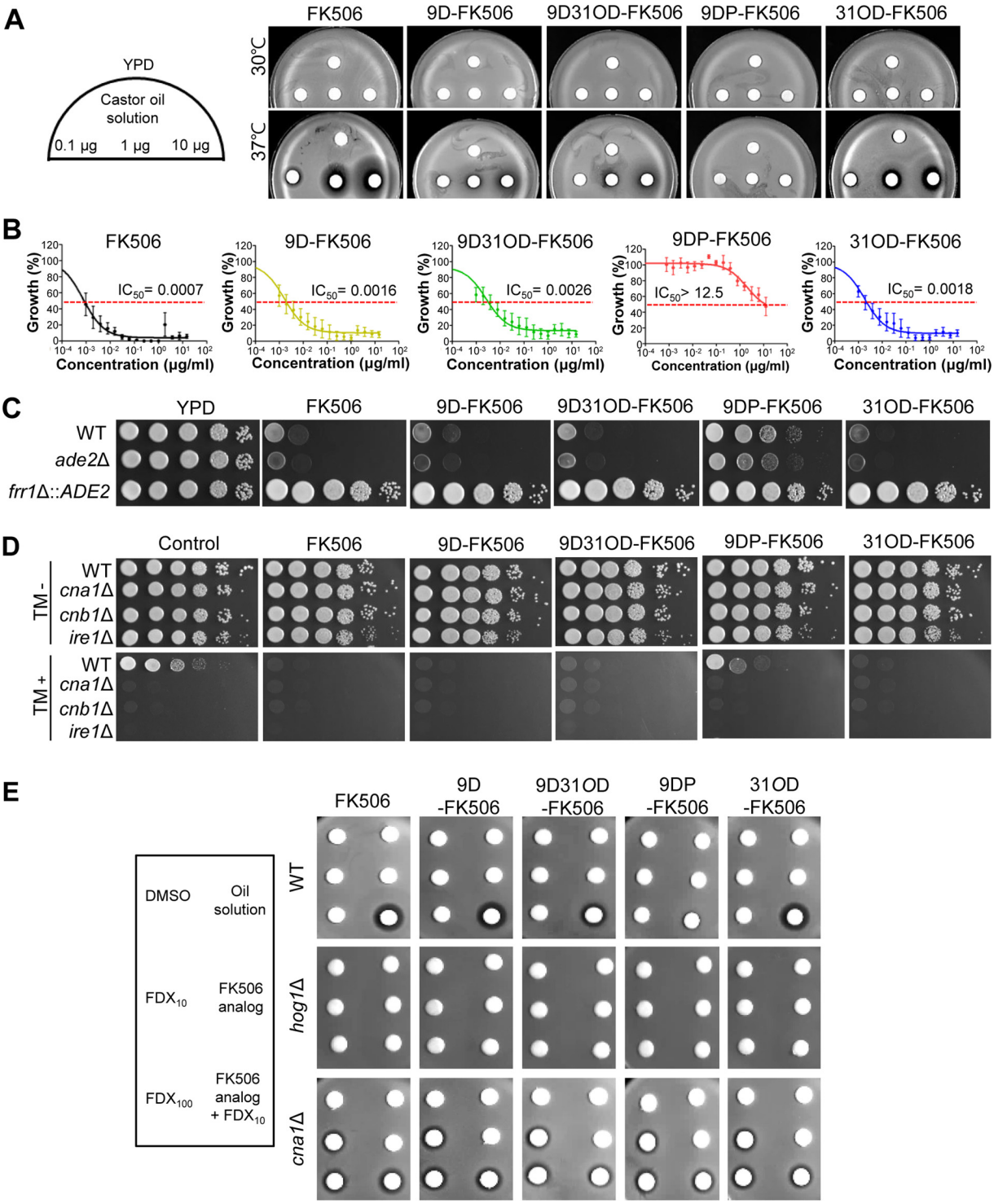

FIG 3 All FK506 analogs, except for 9-deoxo-prolyl-FK506, exhibited dose-dependent antifungal activity against *C. neoformans*. (A) Disk diffusion assays revealed enhanced inhibition of *C. neoformans* with treatment with FK506 and its analogs. A total of 2×10^7 wild-type (H99 strain) cells were resuspended in top agar and poured onto yeast extract-peptone-dextrose (YPD) solid medium. The disks contained 0.1, 1, or 10 μg of FK506 and its analogs. All the FK506 analogs, except for 9DP-FK506, significantly enhanced halo clearing in a concentration-dependent manner at 37°C. (B) MIC test using 2-fold serially diluted FK506 and FK506 analogs from 15 μg/ml. 9D-FK506, 9D31OD-FK506, and 31OD-FK506 suppressed the growth of nine *C. neoformans* isolates. (C) MCC1 (*frr1*::*ADE2* mutant) was resistant to 30 μg/ml of FK506, 60 μg/ml of 9D-FK506, 100 μg/ml of 9DP-FK506, 60 μg/ml of 9D31OD-FK506, and 40 μg/ml of 31OD-FK506, whereas its background strain (*ade2*Δ mutant M049) and H99 cells were susceptible at 37°C. (D) Each *C. neoformans* strain (the H99 wild-type [WT], *cna1*Δ, *cnb1*Δ, and *ire1*Δ strains) was grown overnight, 10-fold serially diluted, and spotted onto YPD medium with or without 1 μg/ml of the FK506 analogs and 0.2 μg/ml of tunicamycin (TM). (E) Synergism between fludioxonil and the FK506 analogs. A disk diffusion assay was performed with FK506, its analogs (4 μg of FK506 and 31OD-FK506 and 6 μg of 9D-FK506, 9DP-FK506, and 9D31OD-FK506), and fludioxonil at 30°C. DMSO, dimethyl sulfoxide; FDX_{10} and FDX_{100}, 10 and 100 μg fludioxonil, respectively.

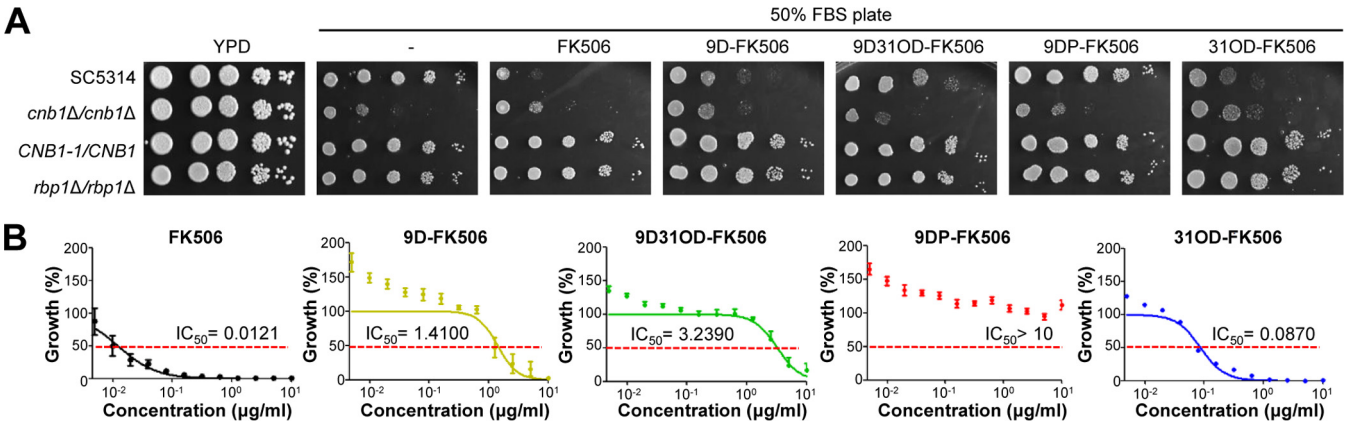

FIG 4 All FK506 analogs, except for 9-deoxo-prolyl-FK506, exhibited antifungal activity against *C. albicans* SC5314. (A) Growth of *C. albicans* (10-fold serially diluted from an OD of 1.0) on 50% FBS agar containing 3 μg/ml of FK506 or its analogs (5 μg/ml 9D-FK506, 10 μg/ml 9D31OD-FK506, 10 μg/ml 9DP-FK506, or 3 μg/ml 31OD-FK506) at 37°C for 24 h. Growth was suppressed compared with that of the nontreated control. All FK506 analogs, except for 9-deoxo-prolyl-FK506, resulted in reduced growth rates over 1 day. (B) MIC test using 2-fold serially diluted FK506 and FK506 analogs from 10 μg/ml.

numbers of CFU mainly resulting from aggregated hyphal formation of *C. albicans* in the presence of serum. The serum-mediated antifungal effect shown by the XTT reduction assay was dose dependent, as reflected by a progressive reduction in cell viability, represented by metabolic activity, with increasing concentrations of FK506 and its analogs. The metabolic activity of *C. albicans* was reduced by 50% at 0.0121 μg/ml of FK506, 1.4100 μg/ml of 9D-FK506, 3.2390 μg/ml of 9D31OD-FK506, and 0.0870 μg/ml of 31OD-FK506 (Fig. 4B; Table 1). In contrast, 9DP-FK506 did not show any activity, even at high doses (Fig. 4B). Taken together, these data show that 31OD-FK506, 9D-FK506, and 9D31OD-FK506, but not 9DP-FK506, exhibit potent *in vitro* antifungal activity through inhibition of the calcineurin pathway in *C. albicans*.

The FK506 analogs exhibit potent *in vitro* antifungal activity against *A. fumigatus*. We next examined the *in vitro* antifungal activity of the four FK506 analogs against the filamentous fungal pathogen *A. fumigatus*. The calcineurin pathway is required for the growth of *A. fumigatus* even at 30°C (48). In agreement with the previous report (48), FK506 was shown to significantly inhibit the growth of *A. fumigatus* at 30°C (Fig. 5A). Similar to the result in *C. albicans*, 31OD-FK506, 9D-FK506, and 9D31OD-FK506, but not 9DP-FK506, significantly reduced the radial hyphal growth of *A. fumigatus* (Fig. 5A). The level of antifungal activity followed the order FK506 > 31OD-FK506 > 9D-FK506 > 9D31OD-FK506. This qualitative measurement was further confirmed by the quantitative measure of the IC_{50} (Fig. 5B). The fungal growth of four clinical isolates of *A. fumigatus* was inhibited by 50% at 0.0313 μg/ml of FK506, 4.6340 μg/ml of 9D-FK506, 19.5500 μg/ml of 9D31OD-FK506, and 0.1797 μg/ml of 31OD-FK506 (Fig. 5B). However, no inhibitory effect was observed with 9DP-FK506, even at high doses. Taken together, these results indicate that 31OD-FK506, 9D-FK506, and 9D31OD-FK506, but not 9DP-FK506, exhibit potent *in vitro* antifungal activity against the filamentous fungus *A. fumigatus*.

Synergistic activity between FK506 analogs and azole drugs. Previously, it has been reported that FK506 has synergism with azole drugs (11, 47, 49). Therefore, we examined whether the FK506 analogs also exhibited synergistic antifungal activity with azole drugs. Similar to FK506, 31OD-FK506, 9D-FK506, and 9D31OD-FK506, but not 9DP-FK506, exhibited a larger halo region with *C. neoformans* when used in combination with voriconazole and fluconazole than when either the FK506 analogs or the azole drugs were used alone (Fig. 6A). Similarly, 31OD-FK506, 9D-FK506, and 9D31OD-FK506 exhibited synergistic antifungal activity against *C. albicans* when used in combination with fluconazole, voriconazole, or itraconazole (Fig. 6B). In particular, 31OD-FK506 presented the most potent synergism with the azole drugs (Fig. 6A and B). In *A. fumigatus*, the FK506 analogs were not significantly synergistic when used with either

TABLE 1 Summary of cytotoxicity, immunosuppressive activity, and antifungal activity of FK506 structural analogs[a]

FK506 analog	Concn for 50% cytotoxicity (μg/ml)	Concn for 50% immunosuppression (ng/ml)	*Cryptococcus neoformans*		*Candida albicans*		*Aspergillus fumigatus*	
			IC_{50} (μg/ml)	Avg IC_{50} (μg/ml)	IC_{50} (μg/ml)	Avg IC_{50} (μg/ml)	IC_{50} (μg/ml)	Avg IC_{50} (μg/ml)
FK506	≃0.001	0.027	0.001	0.0007	0.005	0.01208	0.015	0.0313
9DP-FK506	>1	268.300	4.813	>12.5	322.000	>10	>50.000	>50
9D-FK506	1	0.513	0.039	0.0016	0.963	1.410	24.190	4.6340
31OD-FK506	>1	0.246	0.007	0.0018	0.106	0.08696	0.165	0.1797
9D31OD-FK506	>1	15.090	0.175	0.0026	2.796	3.239	29.770	19.5500

[a]Abbreviations: 9DP-FK506, 9-deoxo-prolyl-FK506; 9D-FK506, 9-deoxo-FK506; 31OD-FK506, 31-*O*-demethyl-FK506; 9D31OD-FK506, 9-deoxo-31-*O*-demethyl-FK506; IC_{50}, 50% inhibitory concentration.

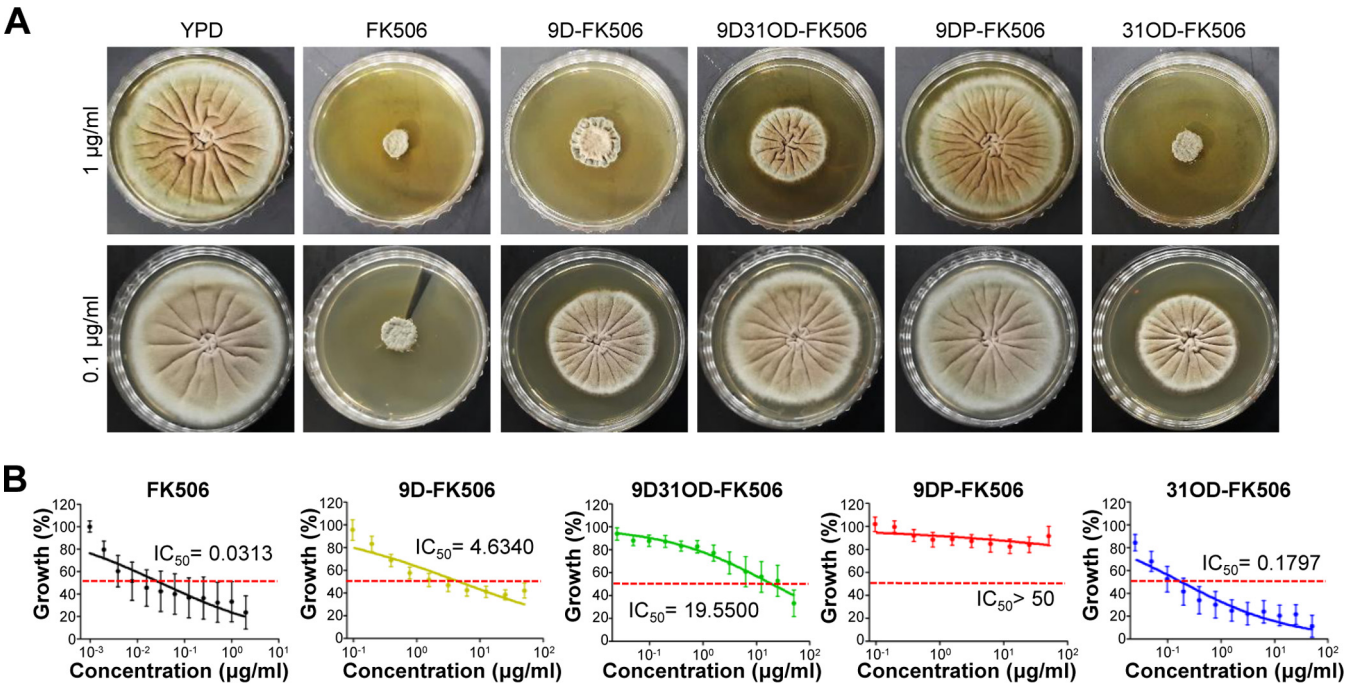

FIG 5 All FK506 analogs, except for 9-deoxo-prolyl-FK506, exhibited antifungal activity against *A. fumigatus* Af293. (A) Growth of *A. fumigatus* (5,000 spores/2 μl) on YPD containing 1 μg/ml of FK506 or its analogs at 37°C for 3 days. The diameter of each colony differed from that of the nontreated control. All FK506 analogs reduced the growth rate across 3 days, except for 9DP-FK506. (B) MIC test using 2-fold serially diluted FK506 and its analogs from 50 μg/ml.

voriconazole or itraconazole (data not shown). Synergism between the FK506 analogs and the azole drugs was further confirmed by a checkerboard assay to determine the fractional inhibitory concentration (FIC) index (Fig. 6C). The calculated FIC index between fluconazole and each FK506 analog was as follows: for FK506, 0.38; for 9D31OD-FK506, 0.31; and for 31OD-FK506, 0.31. Therefore, we confirmed that 9D31OD-FK506 and 31OD-FK506 exhibited synergistic antifungal activity with fluconazole, similar to FK506.

***In vivo* antifungal efficacy of FK506 analogs.** Finally, we examined the *in vivo* antifungal efficacy of the FK506 analogs. First, we utilized an insect model system. The wax moth (*Galleria mellonella*) has been successfully used to monitor the virulence of fungal pathogens. Here, we infected the larvae of *G. mellonella* with *C. neoformans*, subsequently injected 5 mg/kg of body weight of FK506 or its analog at 24, 48, and 72 h postinfection, and then monitored their survival (Fig. 7A). The insects infected with *C. neoformans* and treated with the vehicle died by day 7, whereas noninfected insects showed prolonged survival (40% survival at day 14). We found that insects treated with all four FK506 analogs exhibited prolonged survival compared with nontreated insects, although the efficacy of the FK506 analogs was much lower than that of the control drug, amphotericin B (Fig. 7A).

Of the FK506 analogs studied, we selected 9D31OD-FK506 for further analysis of *in vivo* antifungal efficacy using a murine model of systemic cryptococcal infection, considering its overall cytotoxicity, inhibitory activity on T-cell proliferation, and *in vitro* antifungal activity. Here, we also examined the synergistic *in vivo* antifungal efficacy between 9D31OD-FK506 and fluconazole, based on their *in vitro* synergism, as described above (Fig. 7B). After intravenous infection of female BALB/c mice with the wild-type *C. neoformans* H99 strain, we administered each drug intravenously at a dose of 3 mg/kg at 4, 24, 48, 72, 96, 120, and 144 h postinfection. In contrast to data obtained from the insect model, neither fluconazole nor 9D31OD-FK506 alone was sufficient to treat the cryptococcal infection (Fig. 7B). Interestingly, however, combination treatment with 9D31OD-FK506 and fluconazole significantly extended the survival of the infected mice (Fig. 7B), confirming the synergistic *in vivo* antifungal drug efficacy between these two agents.

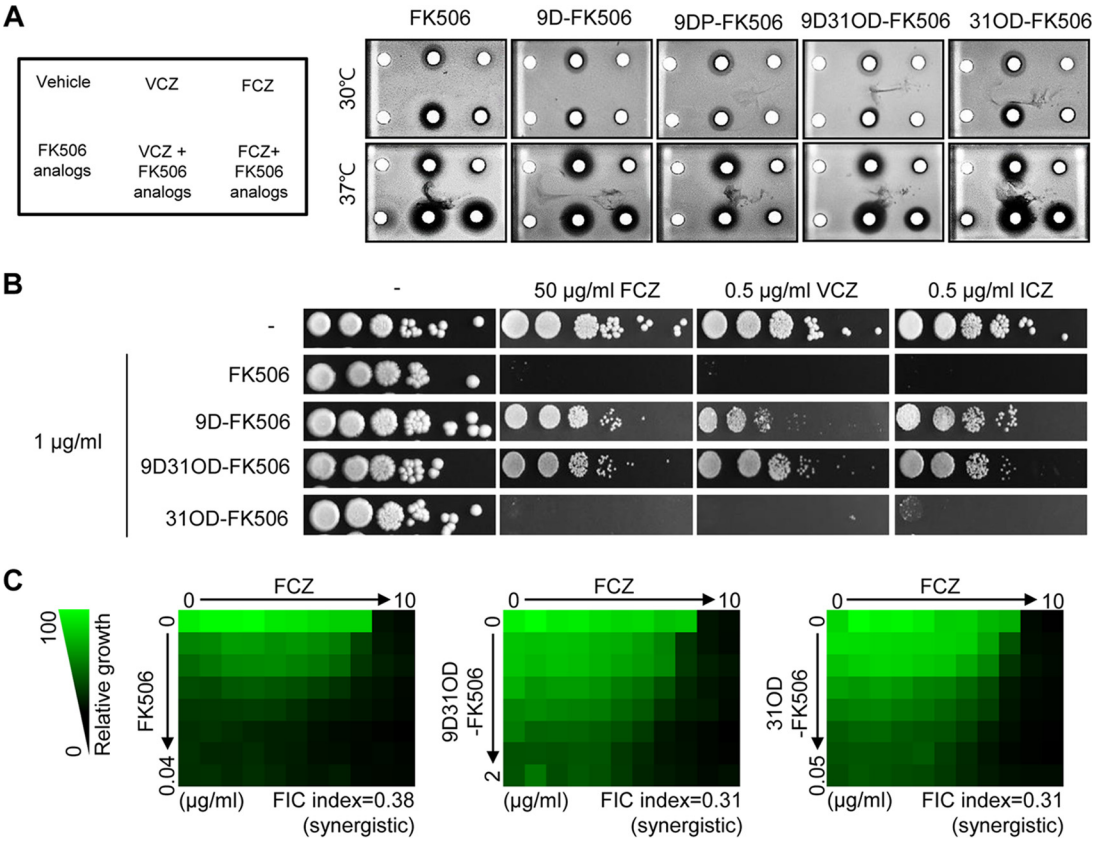

FIG 6 Calcineurin inhibitors exhibited synergistic antifungal activity with azoles against *C. neoformans* and *C. albicans*. (A) Disk diffusion halo assays demonstrated enhanced inhibition of *C. neoformans* when fluconazole and voriconazole were combined with the FK506 analogs. Wild-type (H99) cells were grown in YPD medium overnight. For each strain, 2.5×10^7 cells/ml were resuspended in top agar (10 ml) and poured onto YPD solid medium (20 ml). Cells were incubated for 48 h at 30 and 37°C. FK506 (2 μg) exhibited synergistic antifungal effects at 37°C when combined with 1 μg of voriconazole or 25 μg of fluconazole. Castor oil solution (5 μl) was used as a negative control. (B) *C. albicans* (SC5314) cells were grown in YPD medium overnight. The 2-fold serially diluted cells were spotted onto YPD containing 1 μg/ml of FK506, 9-deoxo-FK506 (9D-FK506), 9-deoxo-31-*O*-demethyl-FK506 (9D31OD-FK506), and 31-*O*-demethyl-FK506 (31OD-FK506) with or without fluconazole, voriconazole, or itraconazole. (C) FIC assay of FK506, 9D31OD-FK506, and 31OD-FK506 with fluconazole. *C. neoformans* cells were grown in YPD medium overnight and diluted in liquid RPMI 1640 medium to 0.01 OD unit/ml. The drugs were 2-fold serially diluted from the indicated concentrations. FCZ, fluconazole; VCZ, voriconazole; ITZ, itraconazole.

DISCUSSION

In this study, we evaluated the potential of a group of FK506 analogs, including 31-*O*-demethyl-FK506 (31OD-FK506), 9-deoxo-FK506 (9D-FK506), 9-deoxo-31-*O*-demethyl-FK506 (9D31OD-FK506), and 9-deoxo-prolyl-FK506 (9DP-FK506), as novel antifungal drugs by examining their cytotoxicity, immunosuppressive activity, and antifungal activities against three major human fungal pathogens, *C. neoformans*, *C. albicans*, and *A. fumigatus* (summarized in Table 1). Among these four analogs, 9DP-FK506 exhibited the greatest reduction in immunosuppressive ability but did not present any significant antifungal activity against the three fungal pathogens tested. In contrast, 9D-FK506 and 31OD-FK506 retained a certain degree of immunosuppressive activity, albeit to a less extent than FK506. In the case of 9D31OD-FK506, which exhibited reduced immunosuppressive activity compared with FK506 (a >100-fold reduction), its antifungal activity was lower than that of FK506, although it retained significant antifungal activity. Therefore, considering both safety and antifungal activity, 9D31OD-FK506 appears to be the preferred choice among the tested FK506 analogs.

The data presented herein provide useful information on the structure-activity relationship (SAR) of FK506 analogs. In both human and fungal cells, FK506 forms a ternary complex with FKBP12 and calcineurin, thereby exerting immunosuppressive and antifungal activity, respectively. Therefore, to develop a nonimmunosuppressive

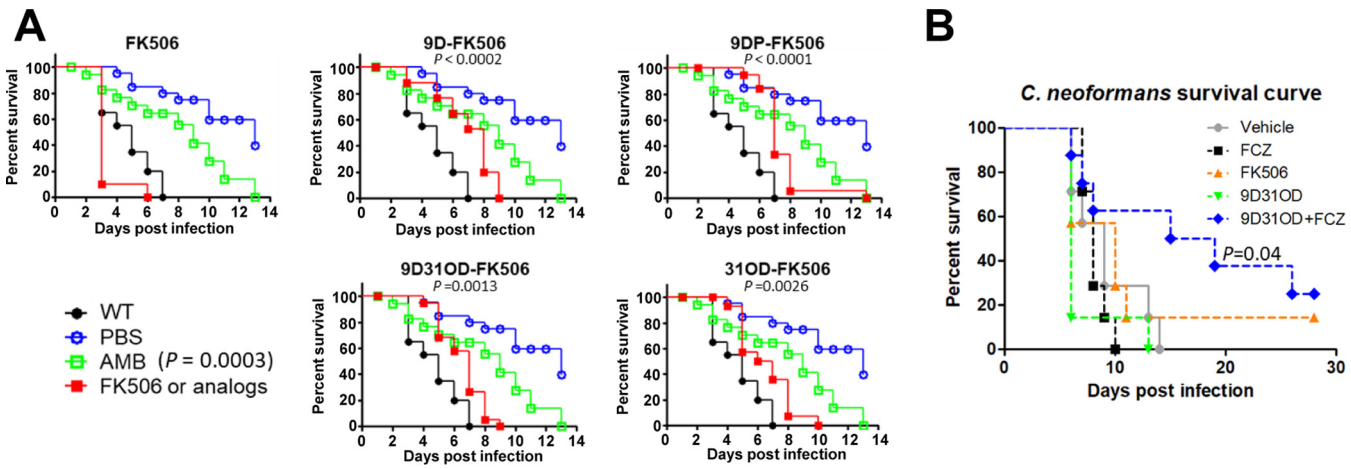

FIG 7 *In vivo* efficacy analysis of the FK506 analogs. The *C. neoformans* cells cultured overnight were washed twice with PBS, and the number of cells was synchronized. (A) *In vivo* efficacy test using a *Galleria mellonella* insect model. Amphotericin B (AMB), FK506, and the FK506 analogs were used at 5 mg/kg, and insects were treated three times at 24, 48, and 72 h after inoculation. (B) *In vivo* efficacy test in a murine model. Cells (5×10^5) were used to infect each mouse via intravenous inoculation. The concentrations of fluconazole (FCZ), FK506, and 9-deoxo-31-*O*-demethyl-FK506 (9D31OD-FK506) were 3 mg/kg, and the combination group was treated with a mixture of 3 mg/kg of 9D31OD-FK506 with 3 mg/kg of FCZ. The log-rank (Mantel-Cox) test was used for statistical analysis.

antifungal agent, the development of an FK506 analog that can discriminate human FKBP12 from fungus or yeast FKBP12 is desirable. However, the structure of the whole protein and the site of interaction with human FKBP (50) are very similar to those of fungi (22) (Fig. 8A), although human FKBP12 shares approximately 50 to 60% sequence identity with fungal FKBP12s (Fig. 8B). Nevertheless, our results suggest that the C-9 and C-31 positions are potential target moieties for the fine-tuning of FK506's affinity toward human and fungal FKBP12s. Substitution of the pipecolinyl ring with a proline at the C-1 position probably affects the binding of FK506 to both human and fungal FKBP12s substantially, leading to a significant reduction in both immunosuppressive and antifungal activities. This observation is supported by the crystal structure, whereby the pipecolinyl ring of FK506 is directly involved in binding to the hydrophobic pocket formed by the Tyr26, Phe46, Trp59, and Phe99 residues in human FKBP12 (Fig. 8C) (50). Interestingly, it has been suggested that replacement of the C-9 carbonyl group, which is also in the proximity of this hydrophobic pocket, with large substituents would drastically reduce human FKBP12 binding, while truncation of the C-9 carbonyl group might restore binding (51). In contrast, the C-31 methyl group of FK506 is outside this hydrophobic pocket (Fig. 8C) (50) and might not significantly affect its binding to FKBP12. Taken together, these structural studies support our observation that the C-9 and C-31 side chains could be potential targets to adjust the affinity of FK506 to FKBP12.

In addition to the FKBP binding region, the calcineurin binding region of FK506 is also critical for modulating its immunosuppressive and antifungal activities. Previously, only the crystal structures of the mammalian ternary complex of FK506, FKBP12, and calcineurin have been reported (52). However, the structure of the fungal ternary complex from *Coccidioides immitis* has recently been reported (PDB accession number 5B8I), which would facilitate the rational design of FK506 analogs that can discriminate human and fungal calcineurins. For example, while Glu54 of FKBP12 forms a hydrogen bond with Gln50 of the calcineurin B subunit in the human ternary complex, Val72 of *C. immitis* FKBP12, which corresponds to Glu54, forms a hydrogen bond with the C-24 hydroxyl group of FK506. This reveals a subtle difference in the binding mode of the FK506-FKBP12 binary complex to calcineurin in humans and fungi, suggesting a further possibility for the synthesis of new FK506 analogs with antifungal activity and no immunosuppressive activity. Currently, we are performing combinatorial biosynthesis of FK506 analogs that contain chemical modifications in the calcineurin binding region as well as in the FKBP binding region.

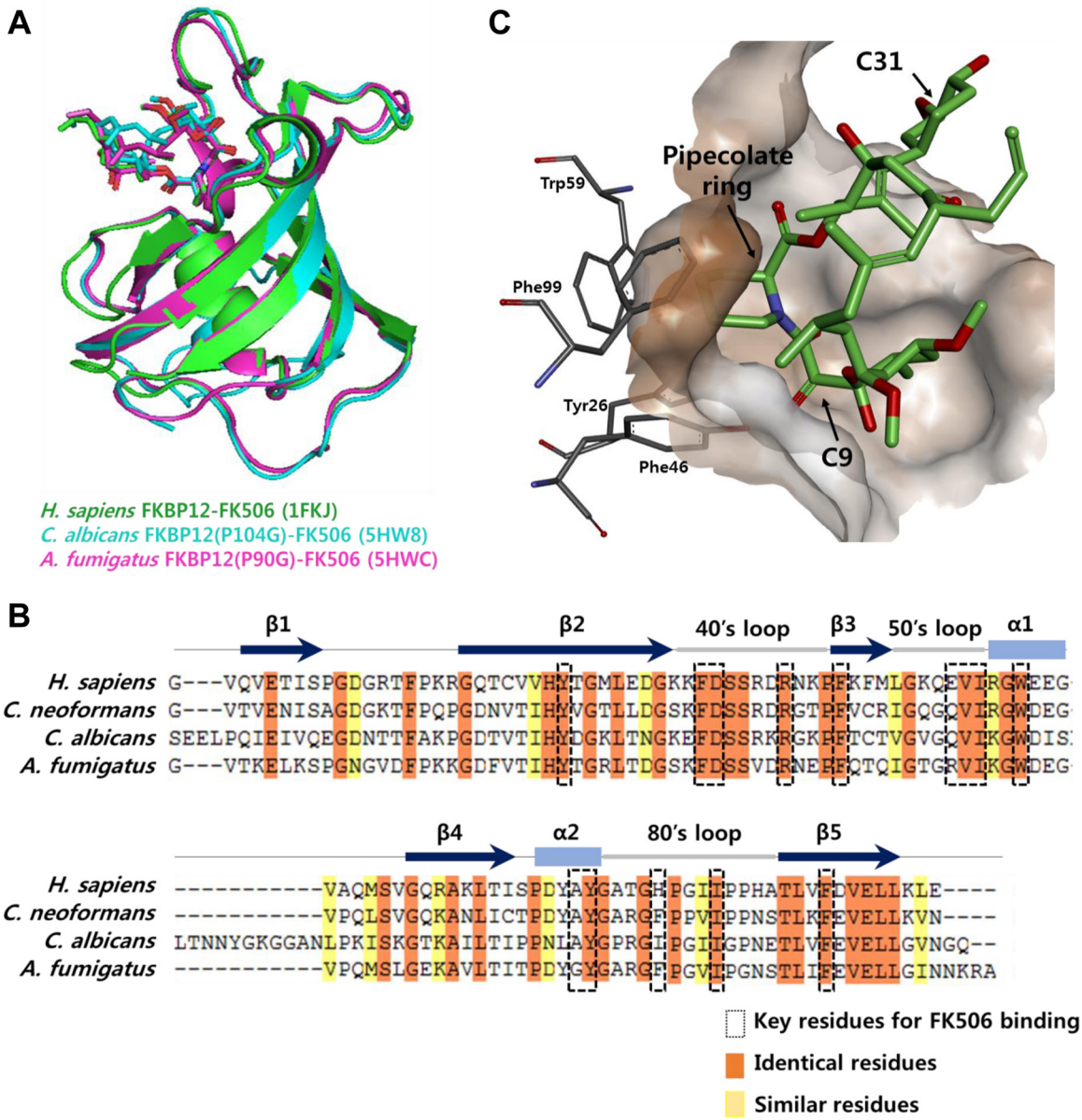

FIG 8 Crystal structures of FKBP12 and alignment of FKBP12 sequences. (A) Superimposition of the FKBP12-FK506 structures of *Homo sapiens* (PDB accession number 1FKJ), *C. albicans* (PDB accession number 5HW8), and *A. fumigatus* (PDB accession number 5HWC). (B) Sequence alignments of the FKBP12s of *H. sapiens*, *C. neoformans*, *C. albicans*, and *A. fumigatus*. The secondary structure of FKBP12 is shown above the sequence. Key residues for binding between FKBP12 and FK506 are labeled with a box. Identical and highly conserved residues are highlighted in orange and yellow, respectively. (C) Binding mode of FK506 within the hydrophobic pocket of human FKBP12 (PDB accession number 1FKJ).

Our *in vivo* efficacy data suggest the potential usefulness of FK506 analogs for further antifungal drug development. As *G. mellonella*, used in the insect model, possesses only an innate immune system (53), we initially expected FK506 to present *in vivo* antifungal efficacy, considering its strong antifungal activity against *C. neoformans* at 37°C. Rapamycin, a previously reported immunosuppressant, effectively inhibited *Mucor circinelloides*, which is another opportunistic fungal pathogen (54). Surprisingly, however, FK506-treated insects died much faster than did nontreated insects, suggesting that FK506 may have intrinsic cytotoxicity even in insects. In contrast, all FK506 analogs that we tested in this study exhibited antifungal efficacy against *C. neoformans*, further verifying their reduced cytotoxicity compared with that of FK506. Nevertheless, in a murine model of systemic cryptococcosis, 3 mg/kg of FK506 or

9D31OD-FK506 was not sufficient for the resolution of cryptococcosis, despite their high *in vitro* antifungal effects. A lack of *in vivo* antifungal efficacy with FK506 or 9D31OD-FK506 alone may be due to their lower bioavailability, as reported for FK506, compared with that of the calcineurin inhibitor cyclosporine in mammals (55). Otherwise, the remaining cytotoxicity or inhibitory activity on T-cell proliferation of 9D31OD-FK506 might still contribute to the reduced survival of infected mice, regardless of the antifungal activity of the FK506 analog. It has also been reported that FK506 alone has no therapeutic activity *in vivo* against *Candida albicans* (56). Nevertheless, here, we found synergism between an FK506 analog and fluconazole, which may be a promising therapeutic option for the treatment of systemic cryptococcosis. The survival rate of mice infected systemically with *C. neoformans* was significantly improved by combination treatment with 9D31OD-FK506 and fluconazole compared with that achieved with either agent alone. As fluconazole has been used as maintenance therapy for recurrent systemic cryptococcosis (57), combination therapy with our lower-immunosuppressive 9D31OD-FK506 may be a useful option to decrease the toxicity and increase the antifungal efficacy of fluconazole.

MATERIALS AND METHODS

Ethics statement. Mice were bred and maintained according to the Institutional Animal Care and Use Committees (IACUC) of Yonsei University, Seoul, Republic of Korea. The Yonsei University IACUC approved all the vertebrate studies.

Preparation of FK506 and FK506 analogs. The FK506 analog compounds were prepared using previously reported procedures (39, 40). Briefly, seed cultures of deletion mutants were prepared in a 250-ml baffled flask containing 50 ml of R2YE medium (39, 40) for 2 days at 28°C. Then, 10 ml of the seed cultures was inoculated into a 3-liter baffled flask containing 1 liter of R2YE medium and grown on an orbital shaker (set at 180 rpm) for 5 days at 28°C. The whole cultures of deletion mutant strains were extracted with twice the volume of ethyl acetate. The organic extract was evaporated to dryness under reduced pressure, and the resultant dark brown residues were separated by open column chromatography with silica gel using methylene chloride and methanol as the mobile phase. These separated fractions were directly injected into a semipreparative high-performance liquid chromatograph (HPLC) to purify the target compounds (55% aqueous acetonitrile solution was used as the mobile phase at a flow rate of 4 ml/min). HPLC purification was performed using Phenomenex (C_{18}; 250 by 10 mm; particle size, 5 μm) columns on an Acme 9000 HPLC system (YL Instrument Co. Ltd.) consisting of an SP930D pump coupled with a UV730D UV detector set to 205 nm and a CTS30 column oven set to 40°C. One milliliter of castor oil solution (dehydrated ethanol:polyethylene glycol 40 castor oil [4:1, vol/vol] [Sigma-Aldrich]) was added to 5.0 mg of powder of each FK506 analog to dissolve the solute. All drugs used in the experiments were prepared using castor oil solution, unless otherwise noted.

***C. neoformans*, *C. albicans*, and *A. fumigatus* strains.** The fungal strains used in this study are shown in Table S1 in the supplemental material. The clinical isolates in Table S1 (marked by shading) were used to obtain the IC_{50}.

Primary immune cell culture. Spleens were dissected from heavily anesthetized B6J male or female mice (age, 6 to 8 weeks) and ground into single cells using a cell strainer, before red blood cells were lysed using ammonium chloride-potassium (ACK) lysing buffer (Gibco). $CD4^+$ T cells were isolated from all lymphocytes using a MagniSort mouse CD4 T-cell enrichment kit (eBioscience). Dynabeads mouse T-activator CD3/CD28 for T-cell expansion (Gibco) were used to activate $CD4^+$ T cells. Cells were incubated for 72 h in 96-well U-bottom culture plates before surface staining and flow cytometry analysis (58).

Surface staining and flow cytometry. A CellTrace Violet (CTV) cell proliferation kit (Molecular Probes) was used to monitor the generations of proliferating T cells. Cells were dyed with CTV according to the manufacturer's instructions on the day of primary immune cell culture. After 72 h of incubation, the cells were surface stained for CD4 markers using Brilliant Violet 605 anti-mouse CD4 antibodies (RM4-5 clone; BioLegend) and CD44 using the activation marker CD44-fluorescein isothiocyanate (BD Biosciences). Cytotoxicity was examined using a LIVE/DEAD fixable near-infrared dead cell stain kit (Molecular Probes). Flow cytometry was performed using a BD FACSCanto II flow cytometer (BD Biosciences). IC_{50} curves were drawn using a nonlinear regression fit with the software Prism.

Disk diffusion halo assays. A wild-type strain (H99) was grown in YPD liquid medium at 30°C overnight. A total of 2×10^7 cells/ml were resuspended in YPD solidified top agar (8 ml) and poured onto YPD solid medium (17 ml). Sterile 6-mm-diameter BBL disks (Becton Dickinson) containing 0.1, 1, and 10 μg of FK506 or the FK506 analogs and 10 μl of castor oil solution (described above) as a negative control were placed over the YPD solidified top agar (59, 60). Cells were incubated at both 30 and 37°C for 48 h and then photographed. For the drug combination halo assay, 2.5×10^7 cells/ml were resuspended in YPD solidified top agar (10 ml) and poured onto YPD solid medium (20 ml). Disks containing 1 μg of voriconazole or 25 μg of fluconazole (Sigma-Aldrich) combined with 2 μg of FK506 or its analogs were placed over the YPD solidified top agar (46, 60, 61).

Growth inhibition assays on solid medium. Qualitative growth inhibition assays were performed with *A. fumigatus* on solid medium, and conidia were adjusted to 5,000 spores/2 μl and spotted onto YPD

solid agar containing 1 μg/ml of FK506 or its analogs. Images were captured after 3 days of growth at 37°C (62).

EUCAST broth microdilution method. All cultures and preparation for MIC and checkerboard assays adhered to EUCAST guidelines, except that 100% FBS (Gibco) was necessary to assess the growth inhibition of *C. albicans* (see "XTT reduction assay" below). A single colony was grown in YPD medium at 30°C for ~20 h and then suspended in liquid RPMI medium (pH 7), which contained 8.4 g RPMI 1640, 34.5 g MOPS (morpholinepropanesulfonic acid), and 20 g dextrose in 1 liter of distilled water. Cells were then added to solutions of FK506 or its analogs as specified above in 96-well microdilution plates to give final suspensions of 100 μl per well at cell densities of 0.01 optical density (OD) unit/ml (63). The inoculated plates were incubated at 35 and 37°C (for *A. fumigatus*, 35°C; for *C. neoformans*, 37°C) for 48 h. The optical density at 600 nm (OD_{600}) was determined with an iMark microplate absorbance reader and was used to determine cell growth. After subtracting the background values for the remaining wells, percent growth relative to the amount of control growth in the absence of inhibitors was calculated under each condition. MICs and fractional inhibitory concentrations (FIC) were calculated as described previously (63, 64).

XTT reduction assay. A wild-type strain (SC5314) was grown in YPD liquid medium overnight. The supernatant was aspirated, and cells were washed twice with phosphate-buffered saline (PBS). Cells (1.25×10^6 cells/ml) were treated with 100% FBS containing FK506 or its analogs in 2-fold serial dilutions from 10 μg/ml and incubated at 37°C for 24 h (30, 31). After 24 h, 500 μg/ml of XTT sodium salt dissolved in PBS was added to 10 μM menadione immediately prior to the assay (XTT solution). Then, 100 μl of the XTT solution was added to each 100-μl well. After 2 h under dark conditions at 37°C, cell survival/proliferation was assessed using the iMark microplate absorbance reader with a wavelength of 490 nm and shaking for 60 s (65).

Determination of FIC index. To quantify the interactions between the antibiotics being tested, the fractional inhibitory concentration (FIC) index value was calculated for each strain and antibiotic combination (64) as follows: FIC = (MIC of drug 1 in the combination/MIC of drug 1 used alone) + (MIC of drug 2 in the combination/MIC of drug 2 used alone), where an FIC of $\leq$0.5 indicates synergy, an FIC of $>$0.5 and $\leq$1.0 indicates an additive effect, an FIC of $>$1.0 and $\leq$2.0 indicates no interaction, and FIC of $>$2.0 indicates antagonism.

Drug susceptibility spotting assay. A *C. albicans* wild-type strain (SC5314) was grown in YPD liquid medium at 30°C overnight. Cultures were adjusted to an OD of 1.0 and serially diluted 10-fold in 96-well microdilution plates. Samples were spotted (3 μl) onto YPD solid medium containing 1 μg/ml of FK506 or its analogs.

***In vivo* antifungal drug efficacy tests.** To test the efficacy of the FK506 analogs against *C. neoformans* infection *in vivo*, the *C. neoformans* H99 strain was grown overnight at 30°C in YPD liquid medium, washed three times with PBS, pelleted, and resuspended in PBS at equal concentrations. The antifungal efficacy of the FK506 analogs was tested *in vivo* using an insect model. We randomly selected a group of 15 *Galleria mellonella* caterpillars in the final-instar larval stage with a body weight of 200 to 300 mg. The insects arrived within 7 days from the day of shipment (Vanderhorst Inc.). A total of 4,000 *C. neoformans* cells in a 4-μl volume per larva were inoculated through the second-to-last proleg using a 100-μl Hamilton syringe equipped with a 10-μl needle and a repeating dispenser (catalog number PB600-1; Hamilton) (66). PBS was injected as a noninfectious control, and treatment with each drug was performed at 24, 48, and 72 h after inoculation. Infected larvae were placed in petri dishes in a humidified chamber, incubated at 37°C, and monitored daily. Larvae were considered dead when a lack of movement was observed when they were touched. Larvae that pupated during the experiments were censored for statistical analysis. *In vivo* antifungal drug efficacy was evaluated using a murine model, in which 7-week-old female BALB/c mice (seven mice per group) were infected intravenously with 5×10^5 cells in 100 μl PBS. Each drug was administered at 4 h postinfection and administered daily from postinfection day 1 to day 6. Mice were housed with free access to food and water under a 12-h light/12-h dark cycle. Mice were checked daily for signs of morbidity (extension of the cerebral portion of the cranium, abnormal gait, paralysis, seizures, convulsion, or coma) and to determine body weight. Mice exhibiting signs of morbidity or significant weight loss were sacrificed with inhalation anesthesia. Each drug was dissolved in castor oil solution and diluted with PBS. Survival curves were generated using Prism (version 6) software (GraphPad). The log-rank (Mantel-Cox) test was used for statistical analysis.

Analysis of crystal structure of FKBP12-FK506 complexes. The superimposition image of the FKBP12-FK506 structures was created by using the free molecular graphics program PyMOL (67). To visualize the molecular surface of the FKBP12-FK506 binding mode, the Protein Data Bank (PDB) format was imported into the BIOVIA Discovery Studio program (68). Multiple-sequence alignment of FKBP12s was carried out by using ClustalX software (69).

SUPPLEMENTAL MATERIAL

Supplemental material for this article may be found at https://doi.org/10.1128/AAC.01627-18.

SUPPLEMENTAL FILE 1, PDF file, 4.1 MB.

ACKNOWLEDGMENTS

This work was supported by the General International Collaborative R&D program, funded by the Ministry of Trade, Industry and Energy (MOTIE) of the Republic of Korea

(N0001720). This work was also supported in part by P01 (P01-AI104533-04) and R01 (R01-AI112595-04) NIH/NIAID grants to J.H., by the Basic Science Research Program through the National Research Foundation of Korea (NRF) funded by the Ministry of Science and ICT (MSIT) (2016R1A2A1A0500507) to Yeo Joon Yoon, and by the Yonsei University Research Fund (Yonsei Frontier Lab Young Researcher Supporting Program to K.-T.L.) of 2018.

We declare that we have no conflicts of interest.

REFERENCES

1. Fisher MC, Henk DA, Briggs CJ, Brownstein JS, Madoff LC, McCraw SL, Gurr SJ. 2012. Emerging fungal threats to animal, plant and ecosystem health. Nature 484:186–194. https://doi.org/10.1038/nature10947.
2. Fones HN, Fisher MC, Gurr SJ. 2017. Emerging fungal threats to plants and animals challenge agriculture and ecosystem resilience. Microbiol Spectr 5(2):FUNK-0027-2016. https://doi.org/10.1128/microbiolspec.FUNK-0027-2016.
3. Hohl TM. 2014. Overview of vertebrate animal models of fungal infection. J Immunol Methods 410:100–112. https://doi.org/10.1016/j.jim.2014.03.022.
4. Brown GD, Denning DW, Gow NA, Levitz SM, Netea MG, White TC. 2012. Hidden killers: human fungal infections. Sci Transl Med 4:165rv13. https://doi.org/10.1126/scitranslmed.3004404.
5. Badiee P, Hashemizadeh Z. 2014. Opportunistic invasive fungal infections: diagnosis & clinical management. Indian J Med Res 139:195–204.
6. Perfect JR, Casadevall A. 2002. Cryptococcosis. Infect Dis Clin North Am 16:837–874, v–vi. https://doi.org/10.1016/S0891-5520(02)00036-3.
7. Musial CE, Cockerill FR, III, Roberts GD. 1988. Fungal infections of the immunocompromised host: clinical and laboratory aspects. Clin Microbiol Rev 1:349–364. https://doi.org/10.1128/CMR.1.4.349.
8. Mesa-Arango AC, Scorzoni L, Zaragoza O. 2012. It only takes one to do many jobs: amphotericin B as antifungal and immunomodulatory drug. Front Microbiol 3:286. https://doi.org/10.3389/fmicb.2012.00286.
9. Fanos V, Cataldi L. 2000. Amphotericin B-induced nephrotoxicity: a review. J Chemother 12:463–470. https://doi.org/10.1179/joc.2000.12.6.463.
10. Kyriakidis I, Tragiannidis A, Munchen S, Groll AH. 2017. Clinical hepatotoxicity associated with antifungal agents. Expert Opin Drug Saf 16:149–165. https://doi.org/10.1080/14740338.2017.1270264.
11. Onyewu C, Blankenship JR, Del Poeta M, Heitman J. 2003. Ergosterol biosynthesis inhibitors become fungicidal when combined with calcineurin inhibitors against *Candida albicans*, *Candida glabrata*, and *Candida krusei*. Antimicrob Agents Chemother 47:956–964. https://doi.org/10.1128/AAC.47.3.956-964.2003.
12. Ryder NS. 1992. Terbinafine: mode of action and properties of the squalene epoxidase inhibition. Br J Dermatol 126(Suppl 39):S2–S7. https://doi.org/10.1111/j.1365-2133.1992.tb00001.x.
13. Hope WW, Tabernero L, Denning DW, Anderson MJ. 2004. Molecular mechanisms of primary resistance to flucytosine in *Candida albicans*. Antimicrob Agents Chemother 48:4377–4386. https://doi.org/10.1128/AAC.48.11.4377-4386.2004.
14. Kahn JN, Hsu MJ, Racine F, Giacobbe R, Motyl M. 2006. Caspofungin susceptibility in *Aspergillus* and non-*Aspergillus* molds: inhibition of glucan synthase and reduction of beta-D-1,3 glucan levels in culture. Antimicrob Agents Chemother 50:2214–2216. https://doi.org/10.1128/AAC.01610-05.
15. Maligie MA, Selitrennikoff CP. 2005. *Cryptococcus neoformans* resistance to echinocandins: (1,3)beta-glucan synthase activity is sensitive to echinocandins. Antimicrob Agents Chemother 49:2851–2856. https://doi.org/10.1128/AAC.49.7.2851-2856.2005.
16. Wang JL, Chang CH, Young-Xu Y, Chan KA. 2010. Systematic review and meta-analysis of the tolerability and hepatotoxicity of antifungals in empirical and definitive therapy for invasive fungal infection. Antimicrob Agents Chemother 54:2409–2419. https://doi.org/10.1128/AAC.01657-09.
17. Nett JE, Andes DR. 2016. Antifungal agents: spectrum of activity, pharmacology, and clinical indications. Infect Dis Clin North Am 30:51–83. https://doi.org/10.1016/j.idc.2015.10.012.
18. De Lucca AJ, Walsh TJ. 1999. Antifungal peptides: novel therapeutic compounds against emerging pathogens. Antimicrob Agents Chemother 43:1–11.
19. Ho S, Clipstone N, Timmermann L, Northrop J, Graef I, Fiorentino D, Nourse J, Crabtree GR. 1996. The mechanism of action of cyclosporin A and FK506. Clin Immunol Immunopathol 80:S40–S45. https://doi.org/10.1006/clin.1996.0140.
20. Skytte DM, Jaroszewski JW, Johansen KT, Hansen SH, Hansen L, Nielsen PG, Frydenvang K. 2013. Some transformations of tacrolimus, an immunosuppressive drug. Eur J Pharm Sci 48:514–522. https://doi.org/10.1016/j.ejps.2012.12.001.
21. Imventarza O, Todo S, Eiras G, Ueda Y, Furukawa H, Wu YM, Zhu Y, Oks A, Demetris J, Starzl TE. 1990. Renal transplantation in baboons under FK 506. Transplant Proc 22:64–65.
22. Tonthat NK, Juvvadi PR, Zhang H, Lee SC, Venters R, Spicer L, Steinbach WJ, Heitman J, Schumacher MA. 2016. Structures of pathogenic fungal FKBP12s reveal possible self-catalysis function. mBio 7:e00492-16. https://doi.org/10.1128/mBio.00492-16.
23. Thomson AW, Bonham CA, Zeevi A. 1995. Mode of action of tacrolimus (FK506): molecular and cellular mechanisms. Ther Drug Monit 17:584–591. https://doi.org/10.1097/00007691-199512000-00007.
24. Bierer BE, Mattila PS, Standaert RF, Herzenberg LA, Burakoff SJ, Crabtree G, Schreiber SL. 1990. Two distinct signal transmission pathways in T lymphocytes are inhibited by complexes formed between an immunophilin and either FK506 or rapamycin. Proc Natl Acad Sci U S A 87:9231–9235.
25. Hamel LP, Nicole MC, Duplessis S, Ellis BE. 2012. Mitogen-activated protein kinase signaling in plant-interacting fungi: distinct messages from conserved messengers. Plant Cell 24:1327–1351. https://doi.org/10.1105/tpc.112.096156.
26. Liu S, Hou Y, Liu W, Lu C, Wang W, Sun S. 2015. Components of the calcium-calcineurin signaling pathway in fungal cells and their potential as antifungal targets. Eukaryot Cell 14:324–334. https://doi.org/10.1128/EC.00271-14.
27. Williamson PR, Jarvis JN, Panackal AA, Fisher MC, Molloy SF, Loyse A, Harrison TS. 2016. Cryptococcal meningitis: epidemiology, immunology, diagnosis and therapy. Nat Rev Neurol 13:13. https://doi.org/10.1038/nrurol.2015.276.
28. Fox DS, Cruz MC, Sia RA, Ke H, Cox GM, Cardenas ME, Heitman J. 2001. Calcineurin regulatory subunit is essential for virulence and mediates interactions with FKBP12-FK506 in *Cryptococcus neoformans*. Mol Microbiol 39:835–849. https://doi.org/10.1046/j.1365-2958.2001.02295.x.
29. Ashman RB, Farah CS, Wanasaengsakul S, Hu Y, Pang G, Clancy RL. 2004. Innate versus adaptive immunity in *Candida albicans* infection. Immunol Cell Biol 82:196. https://doi.org/10.1046/j.0818-9641.2004.01217.x.
30. Ding X, Liu Z, Su J, Yan D. 2014. Human serum inhibits adhesion and biofilm formation in *Candida albicans*. BMC Microbiol 14:80. https://doi.org/10.1186/1471-2180-14-80.
31. Blankenship JR, Wormley FL, Boyce MK, Schell WA, Filler SG, Perfect JR, Heitman J. 2003. Calcineurin is essential for *Candida albicans* survival in serum and virulence. Eukaryot Cell 2:422–430. https://doi.org/10.1128/EC.2.3.422-430.2003.
32. Pierce CG, Chaturvedi AK, Lazzell AL, Powell AT, Saville SP, McHardy SF, Lopez-Ribot JL. 2015. A novel small molecule inhibitor of *Candida albicans* biofilm formation, filamentation and virulence with low potential for the development of resistance. NPJ Biofilms Microbiomes 1:15012. https://doi.org/10.1038/npjbiofilms.2015.12.
33. Blankenship JR, Heitman J. 2005. Calcineurin is required for *Candida albicans* to survive calcium stress in serum. Infect Immun 73:5767–5774. https://doi.org/10.1128/IAI.73.9.5767-5774.2005.
34. Dagenais TR, Keller NP. 2009. Pathogenesis of *Aspergillus fumigatus* in invasive aspergillosis. Clin Microbiol Rev 22:447–465. https://doi.org/10.1128/CMR.00055-08.
35. Falloon K, Juvvadi PR, Richards AD, Vargas-Muniz JM, Renshaw H, Steinbach WJ. 2015. Characterization of the FKBP12-encoding genes in *Asper-*

gillus fumigatus. PLoS One 10:e0137869. https://doi.org/10.1371/journal.pone.0137869.
36. Shirazi F, Kontoyiannis DP. 2013. The calcineurin pathway inhibitor tacrolimus enhances the *in vitro* activity of azoles against *Mucorales* via apoptosis. Eukaryot Cell 12:1225–1234. https://doi.org/10.1128/EC.00138-13.
37. Odom A, Del Poeta M, Perfect J, Heitman J. 1997. The immunosuppressant FK506 and its nonimmunosuppressive analog L-685,818 are toxic to *Cryptococcus neoformans* by inhibition of a common target protein. Antimicrob Agents Chemother 41:156–161.
38. Ban YH, Park SR, Yoon YJ. 2016. The biosynthetic pathway of FK506 and its engineering: from past achievements to future prospects. J Ind Microbiol Biotechnol 43:389–400. https://doi.org/10.1007/s10295-015-1677-7.
39. Ban YH, Shinde PB, Hwang JY, Song MC, Kim DH, Lim SK, Sohng JK, Yoon YJ. 2013. Characterization of FK506 biosynthetic intermediates involved in post-PKS elaboration. J Nat Prod 76:1091–1098. https://doi.org/10.1021/np4001224.
40. Shinde PB, Ban YH, Hwang J-Y, Cho Y, Chen Y-A, Cheong E, Nam S-J, Kwon HJ, Yoon YJ. 2015. A non-immunosuppressive FK506 analogue with neuroregenerative activity produced from a genetically engineered *Streptomyces* strain. RSC Adv 5:6823–6828. https://doi.org/10.1039/C4RA11907J.
41. Nambu M, Covel JA, Kapoor M, Li X, Moloney MK, Numa MM, Soltow QA, Trzoss M, Webb P, Webb RR, II, Mutz M. 2017. A calcineurin antifungal strategy with analogs of FK506. Bioorg Med Chem Lett 27:2465–2471. https://doi.org/10.1016/j.bmcl.2017.04.004.
42. Bedoui S, Heath WR, Mueller SN. 2016. $CD4^+$ T-cell help amplifies innate signals for primary $CD8^+$ T-cell immunity. Immunol Rev 272:52–64. https://doi.org/10.1111/imr.12426.
43. Odom A, Muir S, Lim E, Toffaletti DL, Perfect J, Heitman J. 1997. Calcineurin is required for virulence of *Cryptococcus neoformans*. EMBO J 16:2576–2589. https://doi.org/10.1093/emboj/16.10.2576.
44. Cruz MC, Cavallo LM, Gorlach JM, Cox G, Perfect JR, Cardenas ME, Heitman J. 1999. Rapamycin antifungal action is mediated via conserved complexes with FKBP12 and TOR kinase homologs in *Cryptococcus neoformans*. Mol Cell Biol 19:4101–4112. https://doi.org/10.1128/MCB.19.6.4101.
45. Cheon SA, Jung KW, Chen YL, Heitman J, Bahn YS, Kang HA. 2011. Unique evolution of the UPR pathway with a novel bZIP transcription factor, Hxl1, for controlling pathogenicity of *Cryptococcus neoformans*. PLoS Pathog 7:e1002177. https://doi.org/10.1371/journal.ppat.1002177.
46. Kojima K, Bahn YS, Heitman J. 2006. Calcineurin, Mpk1 and Hog1 MAPK pathways independently control fludioxonil antifungal sensitivity in *Cryptococcus neoformans*. Microbiology 152:591–604. https://doi.org/10.1099/mic.0.28571-0.
47. Cruz MC, Goldstein AL, Blankenship JR, Del Poeta M, Davis D, Cardenas ME, Perfect JR, McCusker JH, Heitman J. 2002. Calcineurin is essential for survival during membrane stress in *Candida albicans*. EMBO J 21:546–559. https://doi.org/10.1093/emboj/21.4.546.
48. Steinbach WJ, Cramer RA, Jr, Perfect BZ, Asfaw YG, Sauer TC, Najvar LK, Kirkpatrick WR, Patterson TF, Benjamin DK, Jr, Heitman J, Perfect JR. 2006. Calcineurin controls growth, morphology, and pathogenicity in *Aspergillus fumigatus*. Eukaryot Cell 5:1091–1103. https://doi.org/10.1128/EC.00139-06.
49. Uppuluri P, Nett J, Heitman J, Andes D. 2008. Synergistic effect of calcineurin inhibitors and fluconazole against *Candida albicans* biofilms. Antimicrob Agents Chemother 52:1127–1132. https://doi.org/10.1128/AAC.01397-07.
50. Van Duyne GD, Standaert RF, Karplus PA, Schreiber SL, Clardy J. 1991. Atomic structure of FKBP-FK506, an immunophilin-immunosuppressant complex. Science 252:839–842. https://doi.org/10.1126/science.1709302.
51. Clackson T, Yang W, Rozamus LW, Hatada M, Amara JF, Rollins CT, Stevenson LF, Magari SR, Wood SA, Courage NL, Lu X, Cerasoli F, Jr, Gilman M, Holt DA. 1998. Redesigning an FKBP-ligand interface to generate chemical dimerizers with novel specificity. Proc Natl Acad Sci U S A 95:10437–10442.
52. Griffith JP, Kim JL, Kim EE, Sintchak MD, Thomson JA, Fitzgibbon MJ, Fleming MA, Caron PR, Hsiao K, Navia MA. 1995. X-ray structure of calcineurin inhibited by the immunophilin-immunosuppressant FKBP12-FK506 complex. Cell 82:507–522. https://doi.org/10.1016/0092-8674(95)90439-5.
53. Mylonakis E, Moreno R, El Khoury JB, Idnurm A, Heitman J, Calderwood SB, Ausubel FM, Diener A. 2005. *Galleria mellonella* as a model system to study *Cryptococcus neoformans* pathogenesis. Infect Immun 73:3842–3850. https://doi.org/10.1128/IAI.73.7.3842-3850.2005.
54. Bastidas RJ, Shertz CA, Lee SC, Heitman J, Cardenas ME. 2012. Rapamycin exerts antifungal activity *in vitro* and *in vivo* against *Mucor circinelloides* via FKBP12-dependent inhibition of Tor. Eukaryot Cell 11:270–281. https://doi.org/10.1128/EC.05284-11.
55. Dheer D, Jyoti, Gupta PN, Shankar R. 2018. Tacrolimus: an updated review on delivering strategies for multifarious diseases. Eur J Pharm Sci 114:217–227. https://doi.org/10.1016/j.ejps.2017.12.017.
56. Chen YL, Lehman VN, Averette AF, Perfect JR, Heitman J. 2013. Posaconazole exhibits *in vitro* and *in vivo* synergistic antifungal activity with caspofungin or FK506 against *Candida albicans*. PLoS One 8:e57672. https://doi.org/10.1371/journal.pone.0057672.
57. Bozzette SA, Larsen RA, Chiu J, Leal MA, Jacobsen J, Rothman P, Robinson P, Gilbert G, McCutchan JA, Tilles J, Leedom JM, Richman DD. 1991. A placebo-controlled trial of maintenance therapy with fluconazole after treatment of cryptococcal meningitis in the acquired immunodeficiency syndrome. N Engl J Med 324:580–584. https://doi.org/10.1056/NEJM199102283240902.
58. Tocci MJ, Matkovich DA, Collier KA, Kwok P, Dumont F, Lin S, Degudicibus S, Siekierka JJ, Chin J, Hutchinson NI. 1989. The immunosuppressant FK506 selectively inhibits expression of early T cell activation genes. J Immunol 143:718–726.
59. Pfaller MA, Diekema DJ, Gibbs DL, Newell VA, Bijie H, Dzierzanowska D, Klimko NN, Letscher-Bru V, Lisalova M, Muehlethaler K, Rennison C, Zaidi M, Global Antifungal Surveillance Group. 2009. Results from the ARTEMIS DISK Global Antifungal Surveillance Study, 1997 to 2007: 10.5-year analysis of susceptibilities of noncandidal yeast species to fluconazole and voriconazole determined by CLSI standardized disk diffusion testing. J Clin Microbiol 47:117–123. https://doi.org/10.1128/JCM.01747-08.
60. Chen YL, Brand A, Morrison EL, Silao FG, Bigol UG, Malbas FF, Jr, Nett JE, Andes DR, Solis NV, Filler SG, Averette A, Heitman J. 2011. Calcineurin controls drug tolerance, hyphal growth, and virulence in *Candida dubliniensis*. Eukaryot Cell 10:803–819. https://doi.org/10.1128/EC.00310-10.
61. Johnson LB, Kauffman CA. 2003. Voriconazole: a new triazole antifungal agent. Clin Infect Dis 36:630–637. https://doi.org/10.1086/367933.
62. Lee SC, Li A, Calo S, Heitman J. 2013. Calcineurin plays key roles in the dimorphic transition and virulence of the human pathogenic zygomycete *Mucor circinelloides*. PLoS Pathog 9:e1003625. https://doi.org/10.1371/journal.ppat.1003625.
63. Singh-Babak SD, Babak T, Diezmann S, Hill JA, Xie JL, Chen YL, Poutanen SM, Rennie RP, Heitman J, Cowen LE. 2012. Global analysis of the evolution and mechanism of echinocandin resistance in *Candida glabrata*. PLoS Pathog 8:e1002718. https://doi.org/10.1371/journal.ppat.1002718.
64. Meletiadis J, Pournaras S, Roilides E, Walsh TJ. 2010. Defining fractional inhibitory concentration index cutoffs for additive interactions based on self-drug additive combinations, Monte Carlo simulation analysis, and *in vitro-in vivo* correlation data for antifungal drug combinations against *Aspergillus fumigatus*. Antimicrob Agents Chemother 54:602–609. https://doi.org/10.1128/AAC.00999-09.
65. Sun S, Li Y, Guo Q, Shi C, Yu J, Ma L. 2008. *In vitro* interactions between tacrolimus and azoles against *Candida albicans* determined by different methods. Antimicrob Agents Chemother 52:409–417. https://doi.org/10.1128/AAC.01070-07.
66. Lee KT, So YS, Yang DH, Jung KW, Choi J, Lee DG, Kwon H, Jang J, Wang LL, Cha S, Meyers GL, Jeong E, Jin JH, Lee Y, Hong J, Bang S, Ji JH, Park G, Byun HJ, Park SW, Park YM, Adedoyin G, Kim T, Averette AF, Choi JS, Heitman J, Cheong E, Lee YH, Bahn YS. 2016. Systematic functional analysis of kinases in the fungal pathogen *Cryptococcus neoformans*. Nat Commun 7:12766. https://doi.org/10.1038/ncomms12766.
67. DeLano LW. 2002. The PyMOL molecular graphics system (2002). DeLano Scientific, Palo Alto, CA. http://www.pymol.org.
68. BIOVIA. 2007. Discovery studio modeling environment, release 4.1. Accelrys Software Inc., San Diego, CA.
69. Thompson JD, Gibson TJ, Plewniak F, Jeanmougin F, Higgins DG. 1997. The CLUSTAL_X windows interface: flexible strategies for multiple sequence alignment aided by quality analysis tools. Nucleic Acids Res 25:4876–4882. https://doi.org/10.1093/nar/25.24.4876.